Development of a 4DoFs exoskeleton robot for passive arm movement assistance

Mohammad H. Rahman*, Thierry K. Ouimet and Maarouf Saad

Electrical Engineering Department,
École de Technologie Superieure,
1100 Notre-dame Ouest, Montreal, Canada
Fax: 514-396-8684
E-mail: mhrahman@ieee.org
E-mail: thierry.kittel@gmail.com
E-mail: maarouf.saad@etsmtl.ca
*Corresponding author

Jean P. Kenné

Mechanical Engineering Department,
École de Technologie Superieure,
1100 Notre-dame Ouest, Montreal, Canada
E-mail: jean-pierre.kenne@etsmtl.ca

Philippe S. Archambault

School of Physical and Occupational Therapy,
McGill University,
3654 Promenade Sir William Osler,
Montreal, Quebec H3G 1Y5, Canada
E-mail: philippe.archambault@mcgill.ca

Abstract: Proper functioning of the upper limbs is important to manage essential activities of daily living. To provide assistance and rehabilitation to individuals with upper limb dysfunction due to conditions such as stroke or spinal cord injuries, we have developed a 4DoFs exoskeleton robot (ExoRob). The ExoRob was designed to be worn on the lateral side of the upper arm, to conform to a naturalistic range of movement for the shoulder and elbow joints. This paper focuses on the modelling, design, development, and control of the ExoRob. Experiments were carried out with healthy human subjects where trajectories tracking in the form of passive rehabilitation exercises were performed. Further experiments were carried out with the master exoskeleton arm (mExoArm, an upper-limb prototype exoskeleton arm) where subjects operate the mExoArm (like a joystick) to maneuver the ExoRob to provide passive rehabilitation. Experimental results show that the ExoRob can effectively perform passive rehabilitation exercises.

Keywords: exoskeleton robot; physical disability; arm impairment; upper extremity rehabilitation; PID control; compliance control; passive arm movements.

Reference to this paper should be made as follows: Rahman, M.H., Ouimet, T.K., Saad, M., Kenné, J.P. and Archambault, P.S. (2012) 'Development of a 4DoFs exoskeleton robot for passive arm movement assistance', *Int. J. Mechatronics and Automation*, Vol. 2, No. 1, pp.34–50.

Biographical notes: Mohammad H. Rahman is with the Electrical Engineering Department, École de technologie supérieure, Université du Québec, Montreal, Canada, on deputation from Khulna University of Engineering and Technology (KUET), Khulna, Bangladesh where he has been serving as an Assistant Professor at the Department of Mechanical Engineering since 2005. He received his BSc in Mechanical Engineering from KUET, Bangladesh in 2001, and his Master of Engineering from Saga University, Japan in 2005. He joined the Department of Mechanical Engineering, KUET in 2001 where he is teaching solid mechanics, CAD, thermal engineering, robotics, control, and machine design courses. His research interests are in bio-robotics, wearable robot, exoskeleton robot, intelligent system and control, nonlinear control, autonomous navigation, artificial intelligence, neural networks, fuzzy systems and control.

Thierry K. Ouimet is an Electrical Engineer. He received his Bachelor and Master's degree in Electrical Engineering from École de Technologie Supérieure respectively in 2009 and 2011, respectively.

Maarouf Saad is a Professor at the Department of Electrical Engineering and Dean of Studies of École de technologie supérieure, Université du Québec, Montreal, Canada. He received his Bachelor and a Master's degree in Electrical Engineering from Ecole Polytechnique of Montreal respectively in 1982 and 1984. In 1988, he received his PhD from McGill University in Electrical Engineering. He joined École de Technologie Supérieure in 1987 where he is teaching control theory and robotics courses. His research is mainly in nonlinear control, and optimisation applied to robotics and flight control system.

Jean P. Kenné is a Professor at the Department of Mechanical Engineering and Director of the Laboratory of Integrated Production Technologies, École de Technologie Supérieure, Université du Québec, Montreal, Canada. He received his Bachelor degree in Mechanical Engineering from the University of Douala (Cameroun) in 1984. He received his Master's and PhD degrees in Mechanical Engineering from Ecole Polytechnique of Montreal respectively in 1991 and 1998, respectively. He has been with GEBO Canada as a Project Manager in Automation at the Digital Control System Department in 1999. He joined the Department of Mechanical Engineering, École de Technologie Supérieure in 2000. His research interests are in capacity planning, control of manufacturing systems and optimisation of production systems performances.

Philippe S. Archambault is an Assistant Professor at the School of Physical and Occupational Therapy, McGill University, and a researcher at the Interdisciplinary Research Center in Rehabilitation (CRIR), Montreal, Canada. He received his undergraduate degrees in Physics and Occupational Therapy from McGill University and his PhD in Neuroscience from the University of Montreal. His research interests are in motor control, technology in rehabilitation, robotics, wheelchair mobility, and virtual reality

1 Introduction

The World Health Organization reports that stroke affects each year more than 15 million people worldwide (Mackay and Mensah, 2004). Among these, 85% of stroke survivors will incur acute arm impairment, and 40% will be chronically impaired or permanently disabled, placing a burden on the family and community (Parker et al., 1986). It is one of the biggest single causes of major disability in the world. Moreover, arm impairment, especially dislocation of shoulder joint is very common due to sports, falls, and occupational injuries (Wilson and Price, 2009). Rehabilitation programmes are the main method to promote functional recovery in these individuals (Heart and Stroke Foundation, 2009), which implies a long commitment by a therapist/clinician or an instructed family member. Since the number of such cases is constantly growing and that the duration of treatment is long, exoskeleton robots could significantly contribute to the success of these programmes, as the proposed *ExoRob* demonstrates to provide passive form of rehabilitation very efficiently, and tirelessly for longer periods of time. Recent studies also revealed that stroke patients who received robot-assisted therapy were able to regain some ability to use their arms, even if the stroke had occurred years earlier (Colombo et al., 2005; Trafton, 2010). For example, researchers at MIT have conducted clinical trials over more than 300 stroke patients since 1991, where the MIT-MANUS, a planar robotic device, was used to provide therapy for shoulder and elbow joint movement (Masia et al., 2007). This approach could significantly reduce arm impairment (Brose et al., 2010; Prange et al., 2006; Volpe et al., 1999, 2003).

1.1 State of the art

To assist physically disabled individuals with impaired upper limb function, extensive research has been carried out, in many branches of robotics, particularly on wearable robot (e.g., exoskeletons, powered orthosis devices etc.) and/or end-effector-based robotic devices (i.e., devices which do not actively support or hold the subject's upper-limb but connect with the subject's hand or forearm (Brose et al., 2010; Burgar et al., 2000; Culmer et al., 2010; Krebs et al., 2000; Loureiro et al., 2003; Takahashi et al., 2008). Note that exoskeleton type robotic devices are either wheelchair mounted (Alexander et al., 1992; Homma and Arai, 1995; Johnson and Buckley, 1997; Tsagarkis and Caldwell, 2003; Rahman et al., 2000; Kiguchi et al., 2003), or floor mounted (Craig et al., 2009; Perry et al., 2007; Frisoli et al., 2009; Rahman et al, 2010; Nef et al., 2009; Gupta and O'Malley, 2006) but the end-effector-based rehabilitative devices are commonly found as floor/desk mounted. Some potential end-effector-based such devices are: MIT-MANUS (a 3DoFs planer robot developed at MIT (Krebs et al., 2000), a later version of which includes hand module for whole arm rehabilitation (Masia et al., 2007); GENTLE/s system (which utilised an active 3DoFs haptic master robot that connects the subject's arm through a wrist orthosis and use virtual reality (VR) technologies to deliver therapy) (Loureiro et al., 2003); iPAM system (developed at the University of Leeds that uses dual robotic arm (each having three active DoFs) to deliver therapy via two orthoses located on the upper arm and wrist of the subjects) (Culmer et al., 2010); MIME system (Burgar et al., 2000) (developed under the joint collaboration of VA Palo Alto

and Stanford University, the system incorporated a PUMA-260 robot and two commercial mobile arm supports modified to limit arm movement to the horizontal plane (2D), a later version of it uses PUMA-560 to provide therapy in 3D workspace); and HWARD (a 3DoFs desk mounted pneumatically actuated device that was developed at University of California to assist subject's hand in grasp and in release movements) (Takahashi et al., 2008).

One of the earliest wheelchair mounted robotic orthosis (developed in mid 60s) was the balanced forearm orthosis (BFO), designed to move subjects' arms in the horizontal planes (Alexander et al., 1992). A later version of the BFO includes an additional joint to allow movement assistance in vertical direction but the device was rarely used due to its poor gravity compensation techniques (Homma and Arai, 1995). Motorised upper-limb orthosis system (MULOS) was also a wheelchair mounted device (having 5DoFs) developed at the University of Newcastle in 1997 (Johnson and Buckley, 1997). Apart from some limitations in safety and control issues, the project seems to be promising but the project ended up in 1997 (Tsagarkis and Caldwell, 2003). Another upper limb motion assist system was developed by Homma and Arai (1995) which used strings to suspend the arm at the elbow and wrist level. Some others wheelchair or chair mounted exoskeleton or orthosis devices developed for upper limb rehabilitation are: the 'rancho golden arm' (Allen et al., 1972) (a 6DoFs device controlled by seven tongue-operated switches was developed at Rancho Los Amigos Hospital); the 'functional upper limb orthosis' (a 4DoFs orthosis developed under the joint project in between Drexel University and A.I. DuPont Hospital for children, was informally tested on ten subjects) (Rahman et al., 2000); the Pneu-WREX (Sanchez et al., 2005) (a 5DoFs pneumatically actuated robot developed at University of California); the Saga University's 'exoskeleton robot for shoulder joint motion assist' (Kiguchi et al., 2003), later version of which was named as SUEFUL-7 having 7DoFs and was controlled by skin surface electromyogram (EMG) signals (Gopura et al., 2009).

Some potential floor mounted (or grounded type) exoskeletons found in recent years are: ABLE (Garrec et al., 2008) (a 4DoFs exoskeleton developed at CEA-LIST, Interactive Robotics Unit, France); CADEN-7 (Perry et al., 2007) (a 7DoFs cable driven exoskeleton developed at University of Washington); L-EXOS (Frisoli et al., 2009) (a 5DoFs force-feedback exoskeleton developed by PERCRO, Italy to provide neuro-rehabilitation in VR environments); 'Soft-actuated exoskeleton' (Tsagarkis and Caldwell, 2003) (a 7DoFs exoskeleton actuated by pneumatic muscle actuators was developed at University of Salford, UK to provide physiotherapy under isokinetic, isotonic and training mode of operation); MGA exoskeleton (Craig et al., 2009) (a 6DoFs exoskeleton designed primarily for shoulder rehabilitation where as a control approach impedance and admittance control scheme were used); ARMin (Nef et al., 2009) (a 6DoFs robot developed at Swiss Federal Institute of Technology, currently under clinical evaluation in hospitals in Switzerland and in the USA); 'Rehabilitation Robot' developed at Okayama University (Noritsugu and Tanaka, 1997) (a 2DoFs robot actuated by pneumatic rubber artificial muscle); and MAHI exoskeleton (Gupta and O'Malley, 2006) (a 5DoFs haptic arm exoskeleton developed at Rice University).

Although much progress has been made in the field of rehabilitation robotics to develop an upper-limb motion assistive robotic device/exoskeleton, we are still far from the desired goal, as existing robots have not yet been able to restore body mobility or function. This is due to limitations in the area of proper hardware design and also of control algorithms to develop intelligent and autonomous robots to perform intelligent tasks. Some limitations of existing exoskeleton systems at the level of hardware can be highlighted as: limited degrees of freedom and range of motion (Alexander et al., 1992; Homma and Arai, 1995; Burgar et al., 2000; Johnson and Buckley, 1997; Noritsugu and Tanaka, 1997; Takahashi et al., 2008; Tsagarkis and Caldwell, 2003; Culmer et al., 2010) compared to that of human upper extremities, robust and complex structure (Tsagarkis and Caldwell, 2003), weak joint mechanisms of the exoskeleton system (Allen et al., 1972; Rahman et al., 2000), bulky actuated joints (Craig et al., 2009), relatively heavy weight of the exoskeleton arm (Noritsugu and Tanaka, 1997; Craig et al., 2009), lack of proper safety measures and compensation for gravity forces (Alexander et al., 1992; Burgar et al., 2000; Culmer et al., 2010; Homma and Arai, 1995; Johnson and Buckley, 1997; Takahashi et al., 2008; Tsagarkis and Caldwell, 2003), and complex cable routing for transmission mechanism (Kiguchi et al., 2003; Perry et al., 2007; Frisoli et al., 2009).

1.2 Contribution to the state-of the art

The *ExoRob* proposed in this research has considered the above limitations and is designed based on the upper-limb joints movement; it has a relatively low weight, an excellent power/weight ratio, can be easily fitted or removed, and is able to effectively compensate for gravity. Moreover to avoid complex cable routing that is found in many exoskeleton systems (Kiguchi et al., 2003; Perry et al., 2007; Frisoli et al., 2009), a novel gear mechanism has been developed for shoulder joint internal/external rotation.

Note that, in our previous research, we have developed an *exoskeleton type robot* for assisting wrist joint movements (Rahman, 2010). In a continuing effort toward the development of a complete upper limb motion assisted (i.e., 7DoFs), exoskeleton robot, in this paper we have focused on the development of a 4DoFs *ExoRob* to provide movement assistance in the human shoulder joint (3DoFs) for horizontal and vertical flexion/extension and internal/external rotation, and in the human elbow joint (1DoF) for flexion/extension motion. Modified Denavit-Hartenberg (DH) conventions were used in developing the kinematic model. In dynamic modelling and control, robot parameters such as robot arm link lengths, upper-limb masses, and inertia, are estimated according to the upper limb properties of a typical adult (Luttgens and

Hamilton, 1997; Winter, 1992; Zatsiorsky and Seluyanov, 1983; Hillman, 2003; Rahman et al., 2009).

The *ExoRob* is supposed to be worn on the lateral side of upper arm with the objective of providing effective rehabilitation for the shoulder and elbow joint movements. The *ExoRob* arm is fabricated with aluminium to provide the structure with a relatively light weight. Brushless DC motors (incorporated with harmonic drives) are used to actuate the proposed *ExoRob*.

The actuation mechanism developed for the shoulder joint internal/external rotation (1DoF) support part is a bit complex, compared to other motions support parts, since it is quite impossible to place any actuator along the axis of rotation of the upper arm (i.e., with the humerus), due to the anatomical configuration of human arm. Although in gear mechanism, actuators can be placed at a certain eccentricity with respect to the desired axis of rotation, such a mechanism is not suitable for our purposes since in such a case, meshing gears are supposed to rotate around a physical axis of rotation (e.g., shaft). We are unable to fit such a mechanical shaft along the line of axis of upper arm motion (i.e., with the humerus). Therefore, we have introduced and developed an alternate gear mechanism, where motion is transmitted from an anti-backlash gear (mounted on a motor shaft) to an open type custom made meshing ring gear that is rigidly attached to the upper arm cup. This gear mechanism is discussed in Section 3.

It is to be noted that, though the proposed *ExoRob* was developed with the goal of providing different forms of rehab therapy (namely *passive arm movements*, *active-assisted therapy*, and *resistive therapy*), in this paper we have focused only on passive form of rehabilitation. Since passive arm movements and exercises are usually performed at natural speed of arm movement or even lower depending on the patient's level of arm impairment, we preferred the simple computationally inexpensive PID controller, rather than complex model-based control algorithms. Moreover, most industrial robots nowadays use this control technique because of problems with having good estimation of dynamic parameters. In fact, it is usually extremely difficult to estimate exact or even good dynamic parameters, especially for the inertial terms (Craig, 2005). In addition, to introduce some compliance in the controller, we have applied a 'compliance control with gravity compensation' technique as an alternative approach to perform similar 'passive form of rehabilitation'.

To evaluate the performance of the proposed *ExoRob*, experiments were carried out with healthy human subjects where typical passive rehabilitation exercises for single and multi joint movements were performed (i.e., pre-programmed trajectory tracking approach). Experiments were also carried out with the *mExoArm* where subjects (robot users) operate the *mExoArm* to trigger the proposed *ExoRob* to provide passive arm therapy. Our experimental results show that the controller is able to manoeuvre the *ExoRob* efficiently to perform a passive rehabilitation protocol for shoulder and elbow joint movements. It is also evident from these results that the proposed *ExoRob* is very efficient to compensate the gravity load that comes from *ExoRob* arm structure and also from the patient's upper limb.

In the next section of this paper, an overview of the development of the kinematic model for the proposed *ExoRob* is presented. Details on its mechanical design and development are presented in Section 3. Section 4 describes the control strategy followed by its electrical and electronic development. In Section 5, experimental results are presented to evaluate the performance of the *ExoRob* regard to passive rehabilitation and finally the paper ends with the conclusion and future works in Section 6.

2 Kinematic model

The proposed *ExoRob* is modelled based on the concept of human upper limb joint motion. Considering user safety and to provide effective rehabilitation, preliminary studies on anatomical range (Luttgens and Hamilton, 1997; Winter, 1992; Zatsiorsky and Seluyanov, 1983; Hillman, 2003) of upper-limb motion has been done to choose a suitable movable range for the *ExoRob*. This movable range is depicted in Figures 1 to 4, and summarised in Table 1.

Figure 1 Movable range of proposed *ExoRob* vertical flexion/extension, (a) initial (zero) position (b) abduction (c) vertical flexion (see online version for colours)

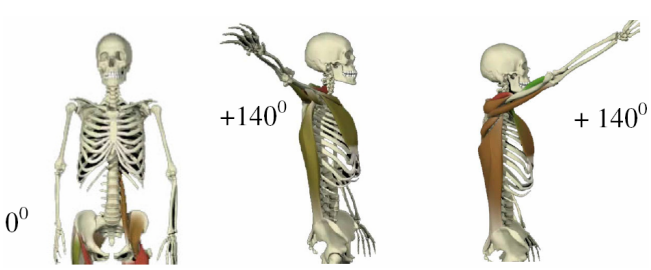

Source: Hillman (2003)

Figure 2 Movable range of proposed *ExoRob,* shoulder joint horizontal flexion/extension, (a) horizontal flexion (b) horizontal extension (see online version for colours)

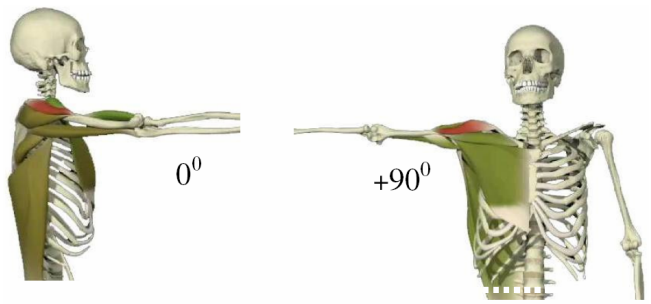

Source: Hillman (2003)

Figure 3 Movable range of proposed *ExoRob,* shoulder joint internal/external rotation, (a) internal rotation (b) initial (zero) position while elbow at position 90° (c) external rotation (see online version for colours)

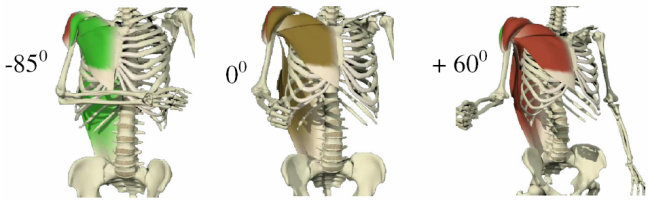

(a) (b) (c)

Source: Hillman (2003)

Figure 4 Movable range of proposed *ExoRob,* elbow joint, (a) initial (zero) position (b) elbow: flexion (see online version for colours)

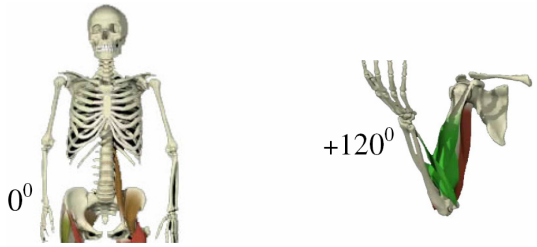

(a) (b)

Source: Hillman (2003)

Table 1 Range of movements

Types of motion	*Anatomical range (Luttgens and Hamilton, 1997)*			*ExoRob's range*
	Source 1	*Source 2*	*Source 3*	
Shoulder joint				
Flexion	180°	170°	180°	140°
Extension	50°	30°	60°	0°
Abduction	180°	170°	180°	140°
Adduction	50°	-	-	0°
Internal rotation	90°	90°	90°	80°
External rotation	90°	90°	60°–90°	60°
Elbow joint				
Flexion	140°	140°	145°	120°
Extension	0°	0°	5°–15°	0°

The link-frame attachments of the *ExoRob*'s kinematic model are depicted in Figure 5. The joint axes of rotation of the human upper limb (as well as that of the *ExoRob*) are indicated by dark black arrows (i.e., Z_i). In this model, joints 1 to 3 constitute the glenohumeral joint (i.e., shoulder joint), where joint 1 corresponds to horizontal flexion/extension, joint 2 represents vertical flexion/extension, and joint 3 corresponds to internal/external rotation of shoulder joint. Note that the axes of rotation of joints 1 to 3 (i.e., $Z_{1–3}$) intersect at a common point located at the centre of rotation of the shoulder joint. For elbow flexion/extension (Z_4), the centre of rotation is located at a certain anatomical distance (d_3, length of humerus) from the shoulder joint. Note that for simplicity of design, the shoulder joint was considered to mechanically resemble a ball-and-socket joint (3DoFs), and the elbow joint is considered as simple hinge joint (1DoF). Though complete shoulder movement also includes scapular elevation that appears due to flexion of the glenohumeral joint (GHJ) or pure scapular elevation without any motion of GHJ, it could be modelled well as a ball-and-socket joint (Perry, Rosen, and Burns, 2007; Craig et al., 2009; Moeslund et al., 2005; Soslowsky et al., 1992) for this application.

Figure 5 Link frame attachments (see online version for colours)

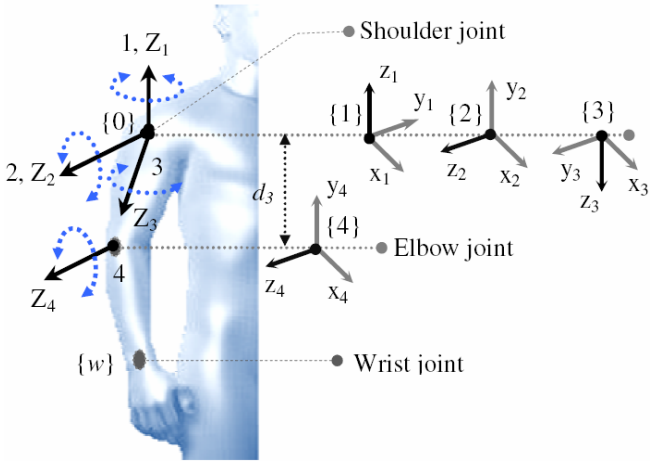

To obtain the DH parameters, we assumed that the coordinate frames (i.e., the link-frames which map between the successive axes of rotation) coincide with the joint axes of rotation and have the same number of order, i.e., frame {1} coincides with joint 1, and frame {2} with joint 2, and so on. The modified DH parameters corresponding to the placement of link frames (in Figure 5) are summarised in Table 2. These DH parameters are used to get a homogeneous transfer matrix which represents the positions and orientations of the reference frame with respect to the fixed reference frame. It is considered that the fixed reference frame {0} coincides with the first reference frame.

Table 2 Modified DH parameters

Joint (i)	α_{i-1}	a_{i-1}	d_i	θ_i
1	0	0	0	θ_1
2	$\pi/2$	0	0	θ_2
3	$\pi/2$	0	d_3	θ_3
4	$-\pi/2$	0	0	θ_4

Note: where α_{i-1} is the link twist, a_{i-1} corresponds to link length, d_i stands for link offset, and θ_i is the joint angle of the *ExoRob.*

We know that the general form of a link transformation that relates frame $\{i\}$ relative to the frame $\{i-1\}$ (Craig, 2005) is

$$ {}^{i-1}_{i}T = \begin{bmatrix} c\theta_i & -s\theta_i & 0 & \alpha_{i-1} \\ s\theta_i c\alpha_{i-1} & c\theta_i c\alpha_{i-1} & -s\alpha_{i-1} & -s\alpha_{i-1}d_i \\ s\theta_i s\alpha_{i-1} & c\theta_i s\alpha_{i-1} & c\alpha_{i-1} & c\alpha_{i-1}d_i \\ 0 & 0 & 0 & 1 \end{bmatrix} \quad (1) $$

Using relation (1), the individual homogeneous transfer matrix that relates two successive frames (of Figure 5) can be written as follows

$$ \begin{aligned} {}^{0}_{1}T &= \begin{bmatrix} c\theta_1 & -s\theta_1 & 0 & 0 \\ s\theta_1 & c\theta_1 & 0 & 0 \\ 0 & 0 & 1 & 0 \\ 0 & 0 & 0 & 1 \end{bmatrix}, \\ {}^{1}_{2}T &= \begin{bmatrix} c\theta_2 & -s\theta_2 & 0 & 0 \\ 0 & 0 & -1 & 0 \\ s\theta_2 & c\theta_2 & 0 & 0 \\ 0 & 0 & 0 & 1 \end{bmatrix} \\ {}^{2}_{3}T &= \begin{bmatrix} c\theta_3 & -s\theta_3 & 0 & 0 \\ 0 & 0 & -1 & -d_3 \\ s\theta_3 & c\theta_3 & 0 & 0 \\ 0 & 0 & 0 & 1 \end{bmatrix}, \\ {}^{3}_{4}T &= \begin{bmatrix} c\theta_4 & -s\theta_4 & 0 & 0 \\ 0 & 0 & 1 & 0 \\ -s\theta_4 & -c\theta_4 & 0 & 0 \\ 0 & 0 & 0 & 1 \end{bmatrix} \end{aligned} \quad (2) $$

The homogenous transformation matrix that relates frame {4} to frame {0} can be obtained by multiplying individual transformation matrices.

$$ \begin{aligned} {}^{0}_{4}T &= {}^{0}_{1}T \cdot {}^{1}_{2}T \cdot {}^{2}_{3}T \cdot {}^{3}_{4}T \\ &= \begin{bmatrix} c\theta_4 s\theta_1 s\theta_3 + c\theta_1 c\theta_2 c\theta_3 - c\theta_1 s\theta_2 s\theta_4 \\ -c\theta_4 c\theta_1 s\theta_3 - c\theta_2 c\theta_3 s\theta_1 - s\theta_1 s\theta_2 s\theta_4 \\ c\theta_2 s\theta_4 + c\theta_3 c\theta_4 s\theta_2 \\ 0 \end{bmatrix} \\ & \quad \begin{matrix} -s\theta_4 s\theta_1 s\theta_3 + c\theta_1 c\theta_2 c\theta_3 - c\theta_1 c\theta_4 s\theta_2 \\ s\theta_4 c\theta_1 s\theta_3 - c\theta_2 c\theta_3 s\theta_1 - c\theta_4 s\theta_1 s\theta_2 \\ c\theta_2 c\theta_4 - c\theta_3 s\theta_2 s\theta_4 \\ 0 \end{matrix} \\ & \quad \begin{bmatrix} c\theta_3 s\theta_1 - c\theta_1 c\theta_2 s\theta_3 & d_3 c\theta_1 s\theta_2 \\ -c\theta_1 c\theta_3 - c\theta_2 s\theta_1 s\theta_3 & d_3 s\theta_1 s\theta_2 \\ -s\theta_2 s\theta_3 & -d_3 c\theta_2 \\ 0 & 1 \end{bmatrix} \end{aligned} \quad (3) $$

The single transformation matrix thus found from relation (3) represents the positions and orientations of the reference frame {4} attached to elbow joint with respect to the fixed reference frame {0}.

Further, considering that frame {*w*} is located at the centre of rotation of the wrist joint, the position and orientation of the wrist joint with respect to frame {0} can be found as follows:

$$ {}^{0}_{w}T = {}^{0}_{4}T \cdot {}^{4}_{w}P \quad (4) $$

where ${}^{4}_{w}P = \begin{bmatrix} x_w & y_w & z_w & 1 \end{bmatrix}^T$ represents the positions of the reference frame {*w*} attached to wrist joint with respect to frame {4} at the elbow joint.

2.1 Singularities

The *ExoRob* arm will be in a singular configuration when it is straight down ($\theta_2 = 0$) by the side (i.e., a singularity will occur when the axes of rotation of joint-1 (Z_1) and joint-3 (Z_3) are aligning about the vertical axis). Note that the joint-space-based control algorithms (that includes both linear and non-linear control techniques, e.g., PID control, computed torque control, sliding mode control) do not require Jacobian matrix or inversion of Jacobian matrix, therefore singularity is not a big issue in this case. On the other hand, Cartesian-based control approaches, which are often used to manoeuvre the manipulator in a straight line motion require Jacobian or inverse Jacobian matrices; therefore for this type of control the singularity must be properly dealt with. Interestingly to replicate these type of trajectories as a rehabilitative exercises e.g., to follow a squared shape trajectory over the surface of a table, the joint-2 (θ_2) usually becomes far away from the singular configuration (i.e., $0° \ll 10° \leq \theta_2 \leq 140° \ll 180°$) of the *ExoRob*. Moreover, as a safety measure when using Jacobian or Cartesian-based control, a singularity could be easily avoided by limiting the movement of joint-2 within 10° to 140° (i.e., $10° \leq \theta_2 \leq 140°$).

3 Exoskeleton robot

The proposed 4DoFs *ExoRob* (as shown in Figure 6) consists of a shoulder motion support part and an elbow motion support part. The entire *ExoRob* arm is fabricated with aluminium to provide the exoskeleton structure with a relatively light weight, considering that aluminium is a low density material having reasonable strength characteristics. The mass and inertia properties of the *ExoRob* are summarised in Table 3. Note that we have used Pro/Engineer software to develop the CAD model as well as to find the mass and inertia parameters of the *ExoRob*.

Table 3 Mass and inertia characteristics of *ExoRob*

Limb segment	*Segment length (m)*	*Segment weight (kg)*	*Moment of inertia I (kg.m²)*		
			Ixx	*Iyy*	*Izz*
Upper arm[a]	0.250	3.45	0.0250	0.0196	0.0124
Elbow[b]	0.267	3.32	0.0341	0.0190	0.0326

Note: [a]Shoulder joint/elbow, [b]elbow/wrist

Figure 6 A 4DoFs *ExoRob* for shoulder and elbow motion assist (see online version for colours)

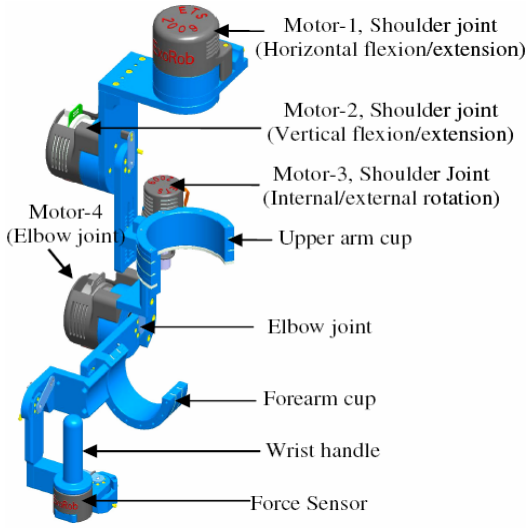

The shoulder joint motion support part has 3DoFs. To assist with horizontal and vertical flexion/extension motion it consists of two motors (Maxon EC-90), two links (link-A, and link-B), and two potentiometers. The link-A holds the motor-1 at its one ends [Figure 7(a)] and is rigidly fixed to the base structure of the robot (not shown in the figures) at its other end. As shown in Figure 7(a), the link-B, which is hinged with the motor-1 and carries the motor-2 on its other end, is 'L' shaped, in order to accommodate the subject's shoulder joint. Therefore, the axes of rotation of motors 1 and 2 are supposed to intersect at the centre of rotation of subject's shoulder joint. Moreover, by adjusting the seating height (e.g., using a height adjustable chair) it would be easy to align the centre of rotation of the shoulder joint of subject to that of the *ExoRob*. It is worth mentioning here that there is no scapular elevation but rather rotation during the abduction of the GHJ (Hallaceli et al., 2004). However, the scapular elevation of subjects which is common due to GHJ flexion will be allowed normally during the vertical flexion motion of the developed *ExoRob* and there will be no discomfort to the subject if the centre of rotation of shoulder joint of the subject aligned with that of *ExoRob*.

Note that motor-1 is responsible for shoulder joint horizontal flexion/extension motion and motor-2 is for vertical flexion/extension motion.

To assist with shoulder joint internal/external rotation, the proposed *ExoRob* is comprised of an upper arm link, a sliding link (link-C), a fixed link (Link-D), a motor (Maxon EC-45), a custom-made open type bearing, a ring gear, an anti-backlash gear and a potentiometer. The upper-arm link as shown in Figure 7(b) is hinged with the motor-2 [Figure 7(a)] and holds the entire *ExoRob* arm. The link-C [Figure 7(a) and 8(a)] is rigidly fixed with the outer circular ring and is able to slide along the upper arm link [Figure 8(a), dotted arrow] so that the distance between the upper arm cup and shoulder joint (as well as the distance between elbow joint and shoulder joint) may be adjusted to accommodate a wide range of users. The outer circular ring, as depicted in Figure 8(b), is designed to hold stainless steel balls (4 mm diameters) on its both sides. Note that the balls are positioned in between the groove of inner and outer circular rings, and act as a frictionless rotating mechanism. The open half-circular structure of the upper arm cup allows users to position the arm easily, without having to insert the arm through a closed circular structure. As depicted in Figure 8 the motor-3 (Maxon EC-45) is rigidly mounted on the back of the fixed outer ring. Figure 8(c) shows the anti-backlash gear which is clamped along the motor shaft to transmit the rotary motion to the ring gear. Note that the open ring gear is firmly fixed to the upper arm cup and is responsible to rotate the upper arm cup over the custom-designed open type bearing.

Figure 7 (a) Shoulder motion support part (b) elbow motion support part (assembled with shoulder joint internal/external rotation support part) (see online version for colours)

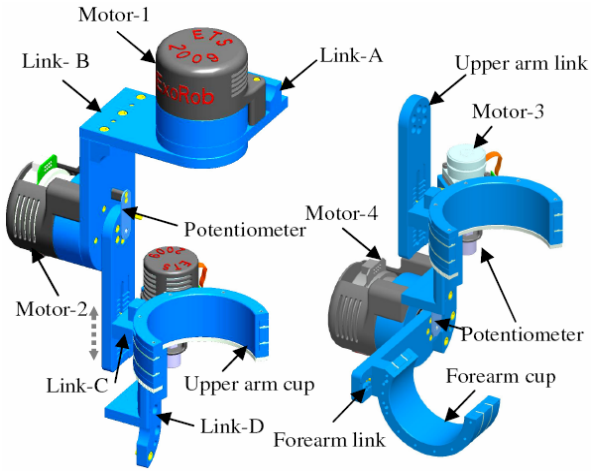

The elbow motion support part is comprised of a forearm link, a fixed link (link-D), a sliding link (link-E), a forearm cup, a motor (Maxon EC-90) and a potentiometer. As shown in Figure 8, the link-D acts as a bridge in between the shoulder joint internal/external rotation support part and the elbow motion support part. Its one end is assembled with the upper-arm cup and with the other end it holds the elbow motor as well as the elbow motion support part of the proposed *ExoRob*. The forearm link as depicted in Figure 8(b) is hinged with the elbow motor at the elbow joint (Figure 6). To hold the forearm in position, a soft arm strap (Figure 9) is pasted on the forearm cup. Like the upper-arm cup, the open half circular structure of the forearm cup allows users to place and position their forearm easily, without having to insert the forearm through a closed circular structure. The sliding link, link-E [Figure 8(a)] is rigidly fixed with the forearm cup [Figure 7(b)] and is able to slide over the forearm link [Figure 8(a), dotted arrow] to adjust the distance between the elbow joint and the forearm strap (as well as to adjust the distance between elbow joint and wrist joint). To hold the upper-arm/forearm in a proper position, soft arm straps (Figure 9) are pasted on the upper-arm and forearm cups.

Figure 8 (a) Shoulder joint internal/external rotation support part (when elbow motor is unplugged from elbow joint) (b) showing custom made open type bearing when upper arm cup is not assembled (c) actuation mechanism for shoulder joint internal/external rotation (d) upper arm cup rotation over custom made bearing (see online version for colours)

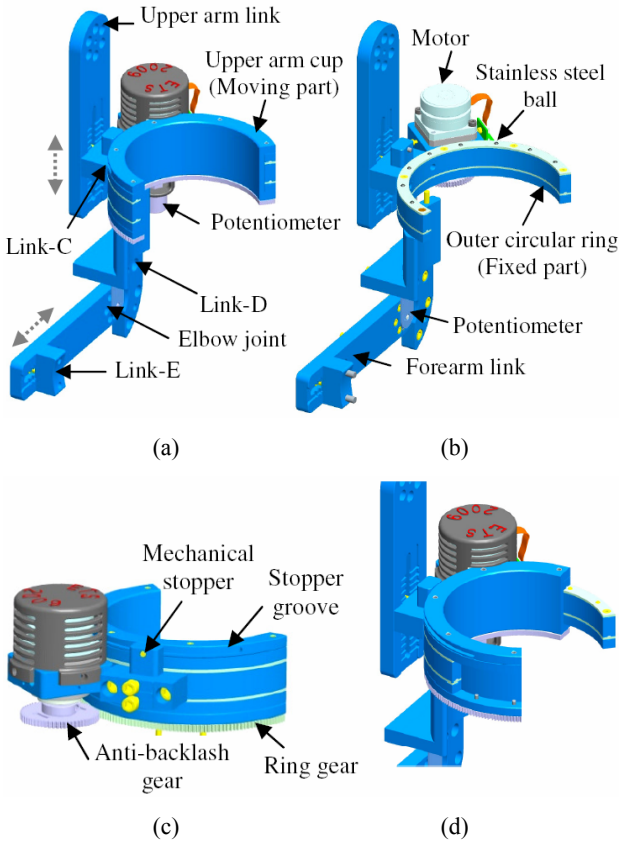

Figure 9 Exoskeleton robot with its user (see online version for colours)

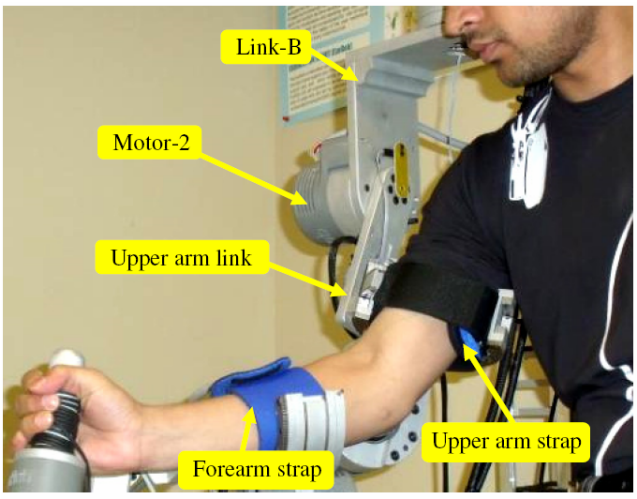

As shown in Figure 6, a high linearity 6-axis force sensor (Nano 17, ATI) is instrumented underneath the wrist handle to measure the instantaneous force feedback. This signal is supposed to be used to actuate *ExoRob* for 'active assist mode of rehabilitation' – *our next step of research*. Note that a sliding link (not shown in the figures) is positioned underneath the force sensor which gives the provision to adjust the distance between wrist joint (of subjects) and wrist handle.

The motors used for this *ExoRob* are brushless DC motors. Harmonic drives (having gear ratio 120:1 for motors 1 and 2 and gear ratio 100:1 for motors 3 and 4) are incorporated with the motors to increase the torque and to reduce the speed of rotation. The specification of motors 1, 2 and 4 are as follows – *nominal speed*: 2,650 rpm, *nominal voltage*: 24 VDC, *no load speed*: 3,190 rpm, *stall torque*: 4,670 mNm; and that for motor 3 is as follows: *nominal speed*: 2,860 rpm, *nominal voltage*: 12 VDC, *no load speed*: 4,400 rpm, *stall torque*: 260 mNm. Note that the potentiometers (as shown in Figures 6 to 9) are incorporated in each joint to measure the angles of rotation.

3.1 Safety issue

As safety measures, mechanical stoppers are added at each joint to limit the angle of rotation within the range of anatomical joints limits (see Table 1, last column). An emergency stop switch is also installed to cut off the power in case if required. As an additional safety measure, the joints' ranges of movements are also limited in the control algorithm.

4 Control

To control the proposed *ExoRob*, as well as to provide passive rehabilitation to upper-extremity, in this paper we have applied a PID control and a compliance control with gravity compensation.

4.1 PID control

The general layout of the PID control technique is depicted in Figure 10. The joint torque commands of the *ExoRob* can be expressed by the following equation.

$$\tau = K_p(\theta_d - \theta) + K_v(\dot{\theta}_d - \dot{\theta}) + K_i\int(\theta_d - \theta)dt \tag{5}$$

where θ_d, $\theta \in \mathbb{R}^4$ are the vectors of desired and measured joint angle respectively, $\dot{\theta}_d$, $\dot{\theta} \in \mathbb{R}^4$ are the vectors of desired and measured joint velocity respectively, K_P, K_V, K_I are the diagonal positive definite gain matrices, and $\tau \in \mathbb{R}^4$ is the generalised torques vector.

Let the error vector E and its derivative be:

$$E = \theta_d - \theta; \quad \dot{E} = \dot{\theta}_d - \dot{\theta} \tag{6}$$

Therefore, equation (5) can be re-formulated as error equation:

$$\tau = K_P E + K_V \dot{E} + K_I \int E dt \tag{7}$$

The relation (7) is decoupled therefore individual torque command for each joint would be as follows.

$$\tau_i = K_{P_i} e_i + K_{V_i} \dot{e}_i + K_{I_i} \int e_i dt \tag{8}$$

where $e_i = \theta_{d_i} - \theta_i \ldots (i = 1, \ldots, 4)$; θ_i, θ_{d_i} are the measured and desired trajectory for joint i respectively, and

$$\dot{E} = \begin{bmatrix} \dot{e}_1 & \dot{e}_2 & \dot{e}_3 & \dot{e}_4 \end{bmatrix}^T, \quad \theta_d = \begin{bmatrix} \theta_{d_1} & \theta_{d_2} & \theta_{d_3} & \theta_{d_4} \end{bmatrix}^T,$$

$$\theta = \begin{bmatrix} \theta_1 & \theta_2 & \theta_3 & \theta_4 \end{bmatrix}^T, \quad K_P = diag\begin{bmatrix} K_{P_1} & K_{P_2} & K_{P_3} & K_{P_4} \end{bmatrix},$$

$$K_V = diag\begin{bmatrix} K_{V_1} & K_{V_2} & K_{V_3} & K_{V_4} \end{bmatrix} \text{ and}$$

$$K_I = diag\begin{bmatrix} K_{I_1} & K_{I_2} & K_{I_3} & K_{I_4} \end{bmatrix}.$$

Figure 10 Schematic diagram of PID control (see online version for colours)

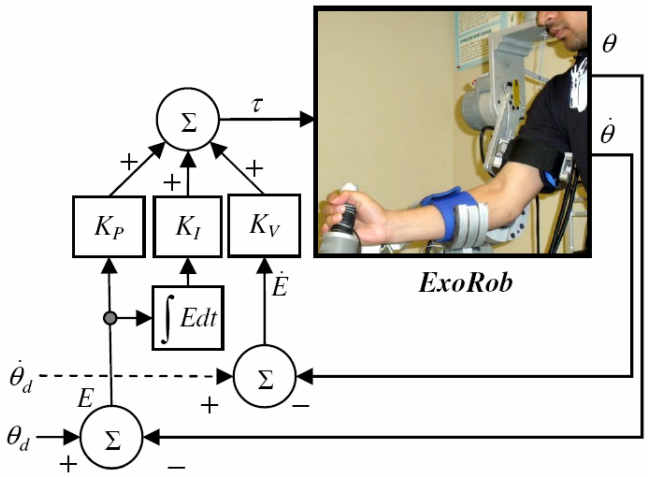

4.2 Compliance control with gravity compensation

The gravity model of a manipulator is often added to the control law to realise the simple model-based control (Craig, 2005) as well as to minimise the static position error. One of the existing techniques of gravity compensation is the addition of a gravity model with a control law, such as with a PID control law as found in Craig (2005) and Yang et al. (2011). De Luca et al. (2005) proposed similar technique for the gravity compensation but with the PD control law. Both approaches mentioned above, work on the stiff position control which sometimes the cause of an end-effector being jammed or damaged when it interacts with the environment. As a solution to this problem, Salisbury (1980) proposed an active stiffness control technique where the position gain (K_p) of a joint-based control system was modified to provide some stiffness to the end-effector along the Cartesian degree of freedom (Craig, 2005; Salisbury, 1980). Later, Craig (2005) implements this concept with a PD control law, where the position gain of the controller was modified as proposed by Salisbury (1980). However, in this paper, we proposed a modified version of compliance control technique that combined the concept of softening position gains (Salisbury, 1980) and the gravity weight compensation (Craig, 2005). Therefore, the gravity model of the *ExoRob* was included in the control law. The general layout of the proposed control scheme is depicted in Figure 11. Unlike the compliance technique suggested by Salisbury (1980) and Craig (2005) we have added an integral term to obtain a better tracking performance as well as to minimise the steady state error.

Figure 11 Schematic diagram of compliance control with gravity compensation (see online version for colours)

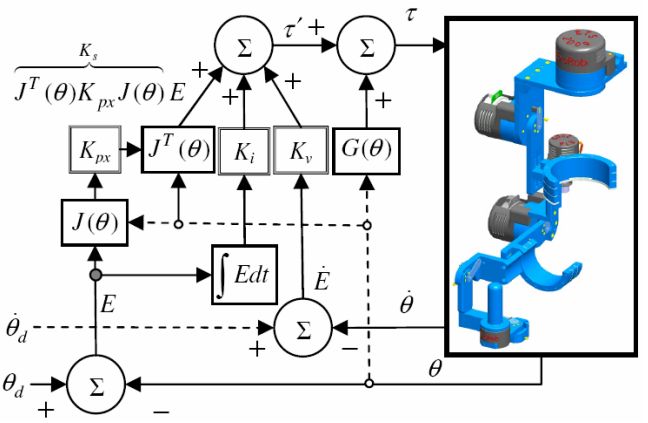

We know that the stiffness characteristics of a spring can be expressed by the following equation.

$$F = K_{px} \cdot \Delta x \tag{9}$$

where $\Delta x \in \mathbb{R}^{6\times1}$ is the generalised displacement vector, $F = [f_x \; f_y \; f_z \; \tau_{xy} \; \tau_{yz} \; \tau_{zx}]^T \in \mathbb{R}^{6\times1}$ is the force and torque vector, and $K_{px} \in \mathbb{R}^{6\times6}$ is the positive definite diagonal matrix known as spring constant having three linear stiffness in X, Y, and Z directions followed by three rotational stiffness in XY, YZ and ZX planes.

Using the definition of Jacobian (Schilling, 1990), we may write:

$$dx = J(\theta) d(\theta) \tag{10}$$

where $J(\theta) \in \mathbb{R}^{6\times n}$ is the manipulator Jacobian matrix, and dx, $d\theta$ represent the infinitesimal displacement of tool and joints, respectively.

Now, if the tool (end-effector) deflection, Δx and corresponding joint deflection $\Delta\theta$ are small enough, i.e., approaching infinitesimal, then we can equate Δx with dx, and $\Delta\theta$ with $d\theta$ (Schilling, 1990), and thus equation (10) can be rewritten as:

$$\Delta x = J(\theta)\Delta(\theta) \tag{11}$$

Combining relations (9) and (11), we have

$$F = K_{px} J(\theta)\Delta(\theta) \tag{12}$$

Therefore, considering a static force F applied to the end-effector, the joint torques can be computed easily by,

$$\tau = J^T(\theta)F = \underbrace{J^T(\theta)K_{px}J(\theta)}_{K_s}\Delta(\theta) \tag{13}$$

where K_s is the joint space stiffness matrix. Note that the Jacobian is written here in the end-effector frame which transforms the Cartesian stiffness to the joint space stiffness. Therefore, equation (13) represents the required joint torques (τ) that should be applied due to a change of joint angles ($\Delta\theta$) so that the end-effector behaves as a Cartesian spring (in 6DoFs) which a spring constant denoted as: $K_{px} \in \mathbb{R}^{6\times6}$ (Salisbury, 1980).

The control law as seen from Figure 11 can be expressed by the following relation.

$$\tau = \overbrace{J^T(\theta)K_{px}J(\theta)}^{K_s} E + K_v\dot{E} + K_i\int Edt + G(\theta) \tag{14}$$

where $G(\theta) = (\partial P_g(\theta)/\partial\theta)^T$ is the $n \times 1$ gravitational vector, and $P_g(\theta)$ is the potential energy due to gravity (Craig, 2005). So, the gravity term $G(\theta)$, contains the mass and link length properties (i.e., the vector locating the centre of mass of each link) of the *ExoRob*.

Comparing equations (7) and (14), it is evident that control law for the developed compliance control technique is quite similar to the joint-based position controller; except for the position gain [K_p, of equation (7)] which was modified to form a joint stiffness matrix [K_s, of equation (14)] so that the end-effector exhibits some spring characteristics along the Cartesian degree of freedom (Craig, 2005; Salisbury, 1980).

Note that the control gains K_P, K_V, K_I (of PID control) and K_{px}, K_v, K_i (of compliance control) are positive definite matrices. A proper choice of these matrices ensures the stability of the system (Rocco, 1996; Alvarez-Ramirez et al., 2000).

4.3 Development of electrical and electronic component

The electrical and electronic configuration for the proposed exoskeleton robot system is depicted in Figure 12. It consists of a CompactRIO (NI cRIO-9074), a main board, motor driver cards, and a host PC.

The NI cRIO-9074 is an integrated system that combines a real-time processor, 128 MB of DRAM, 256 MB of non-volatile memory, and a reconfigurable field-programmable gate array (FPGA) for embedded machine control and data logging (National Instruments, 2010). The unit has two Ethernet ports (10/100 Mb/s) and a RS232 port, which is used here for communication with the host PC via TCP/IP protocol. The input/output modules used with cRIO-9074 unit were NI-9205, analogue input module (*spec*: 16-bit, 32 channels, ± 10 V); NI-9264, analogue output module, (*spec*: 16-bit, 16 channels, ± 10 V); and NI-9403, digital I/O module (32 channels).

The main board as shown in Figure 12 acts as a mother board and is powered by AC 120 V (60 Hz) supply. The mother board routes various analogue and digital signals from/to cRIO-9074 to the *ExoRob* system. For instance, it routes analogue inputs (from potentiometer and current feedback) to NI-9205 module; analogue outputs (e.g., motor driver reference voltage) from NI-9264 module; and digital outputs (e.g., to activate the motors, relay switch control, etc.) from NI-9403 module to the *ExoRob* system. The board as shown was designed to have slots for motor driver cards, only one of which was depicted in Figure 12. Note that as a safety features emergency stop switch was installed with the board to cut-off the power in case any emergency. In addition a safety fuse of 6 A was also used to protect different electrical/electronic components.

Motor driver cards which carry the motor drivers (ZB12A8) were custom designed to fit in the slots of main board. The drivers used are type of PWM servo amplifiers specially designed to drive brushless DC motors at high switching frequency 33 kHz (*spec*: reference voltage: ± 15 VDC analogue output ± 10 VDC, maximum continuous current: ± 6 A). Note that, to double the safety features safety fuses of 3 A were installed in each of the motor driver cards.

Note that the control architecture of the PID control and compliance control techniques as well as all programme code (I/O communication) was built in the LabVIEW environment (National Instruments, USA). The host PC as depicted in the schematic (Figure 12) is for the display purpose (e.g., joint's position, velocity, torque etc.) only.

Potentiometers at each joint are sampled at 0.2 ms. The signals are then filtered (second order filtering: $\omega_0 = 30$, $\zeta = 0.9$) prior to be sent to the controller. Filtering is important to eliminate high frequency or noisy data from the desired signals. Velocity of joints is found easily from the output vector of second order filtering (Figure 13). Note that the both PID and compliance controller updates the torque commands to the motor driver at each 2 ms and is executed in FPGA of NI cRIO-9074.

5 Experiments

Experiments were carried out with healthy human subjects (age: 24 to 34 years, height: 163 to 177 cm, weight: 54 to 118 kgs) to provide passive rehabilitation involving shoulder and elbow joint movements. This included horizontal and vertical flexion/extension of the shoulder joint, internal/external rotation of the shoulder joint, flexion/extension of the elbow joint, and multiple joint movements (e.g., reaching). As depicted in Figure 9, the *ExoRob* arm is worn on the lateral side of seated subjects arm. Since the proposed *ExoRob* is mounted on a rigid base structure on the floor, wearing the *ExoRob* will not impinge any load to the subject. Further, the control algorithm is designed to compensate gravity loads efficiently and smoothly (mass of the *ExoRob* arm and that of the upper limb).

Figure 12 Schematic diagram of electrical and electronic configuration

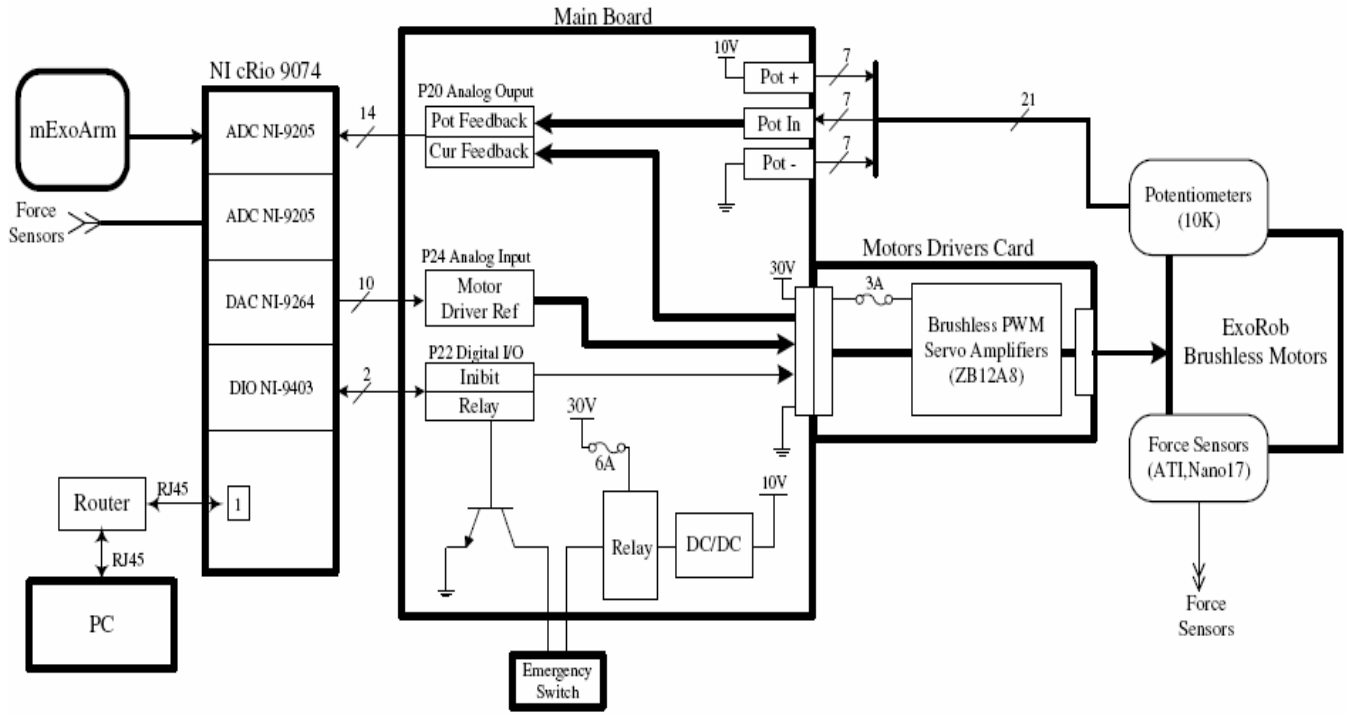

Figure 13 Schematic diagram of 2nd order filtering (see online version for colours)

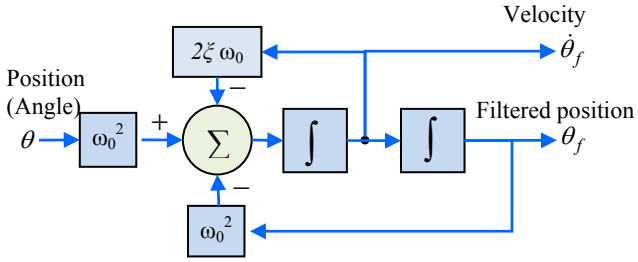

Figure 14 A 7DoFs upper-limb prototype *mExoArm*, (a) left-front view (initial position) (b) joints 1 and 2 are rotated to 30°, joint 3 is to 60° and joint 4 is to 70° (c) *mExoArm* after fabrication (see online version for colours)

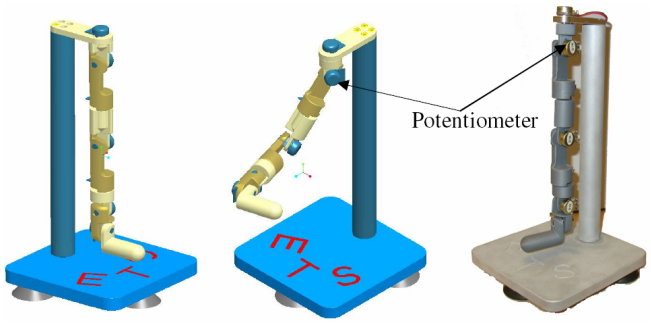

(a) (b) (c)

5.1 Experimental results with PID control

In experiments we introduced two options for providing passive therapy. In the first option, the *ExoRob* was manoeuvred to follow a pre-programmed trajectory that corresponds to recommended passive rehab protocol (Brigham and Women's Hospital, 2010; Inverarity, 2008). For the second option, using the *mExoArm* (Figure 14) users has the flexibility to replicate different rehab trajectories promptly according to his/her requirements to manoeuvre the *ExoRob*. It is assumed that users (patients) can operate the *mExoArm* with their good (functional) hand, or alternatively, that it can be operated by a family member or caretaker. Using *mExoArm* provides flexibility in choosing the range and speed of movements and as well as the ability to provide motion assistance.

5.1.1 Passive rehabilitation using pre-determined exercises

The intent of this protocol was to provide rehabilitation at the level of the shoulder and elbow joints from a library of passive rehabilitation exercises, which was formed according to recommended passive therapy protocols (Brigham and Women's Hospital, 2010).

Figure 15 shows the experimental results of shoulder joint vertical flexion/extension motion where the *ExoRob* raises the subject's arm [from the initial position, Figure 1(a)] to a specific position over the head [e.g., in Figure 15(a), the elevation was set at 130°], hold that position for a few seconds [e.g., in Figure 15(a), 4 sec.] and then slowly move the joint back to its initial position. The topmost plot of Figure 15 compares the desired joint angles (or reference trajectories, dotted line) to measured joint angles (or measured trajectories, solid line). It is obvious from the figure that the controller's performance was excellent since measured trajectories overlapped with the desired trajectories. The intermediate plot of Figure 15 shows the

error as a function of time (i.e., deviation between desired and measured trajectories). It can be seen that the tracking error was quite small (<2°) and that the most noticeable one was the steady state error (i.e., when *ExoRob* is maintaining the position at 130° against gravity) which lies below and/or near around 0.1°. Note that two spikes as apparent in the error plots; these are due to static friction that has a large value during the initiation of the upward [where error was around 3°, Figure 15(a)] and the downward movement [e.g., in Figure 15(a), downward movement starts from 130°, where deviation was around 4°]. The generated joint torques corresponding to the trajectory are plotted in the bottom row of Figure 15.

Passive forward elevations at different joint angles are depicted in Figures 15(b) to 15(d). These exercises are also known as pointing movements, with the goal of gradually increasing passive ROM.

Figure 16 shows a passive horizontal flexion/extension motion of the shoulder joint, where passive forward elevation (i.e., vertical flexion of shoulder joint) is maintained at 90°. Again, the tracking performance of the controller was excellent, with tracking error less than 2° and the steady state position error below 0.05°.

Figure 17 demonstrates a cooperative movement of the elbow (flexion/extension) and shoulder joint internal/external rotation. The objective of this exercise is to provide repetitive movement at the level of the shoulder joint while maintaining the elbow at 90°. As shown in Figure 17(a) the exercise begins with elbow flexion, then repetitive internal/external rotation was performed [Figure 17(b)]; finally the exercise ends with the extension of the elbow to 0° [Figure 17(a)]. The 3rd row of the plots (from the top) displays velocity tracking, where it can be seen that the measured velocity (solid line) nicely overlapped with the desired velocity (dotted line), thus demonstrating the excellent performance of the controller with respect to both position and velocity tracking.

It is recommended to maintain shoulder joint vertical flexion at 90° while performing passive shoulder joint horizontal flexion/extension, and likewise, the elbow at 90° while performing internal/external rotation. However, it is evident from our results that *ExoRob* users can do the same passive arm movements, in any position of elbow and shoulder elevation (depending on the physical condition of patient). Moreover, these results also demonstrate that the *ExoRob* is able to compensate the gravity effect which is very much important for this type of robotic applications as well as to provide passive arm therapy.

Figure 15 Shoulder joint vertical flexion/extension motion, (a) passive forward elevation up to 130° (b) passive forward elevation up to 120° (c) passive forward elevation up to 90°, showing a fast movement compare to other exercises where tracking performance of the *ExoRob* is also found quite good (d) passive forward elevation up to 60° (see online version for colours)

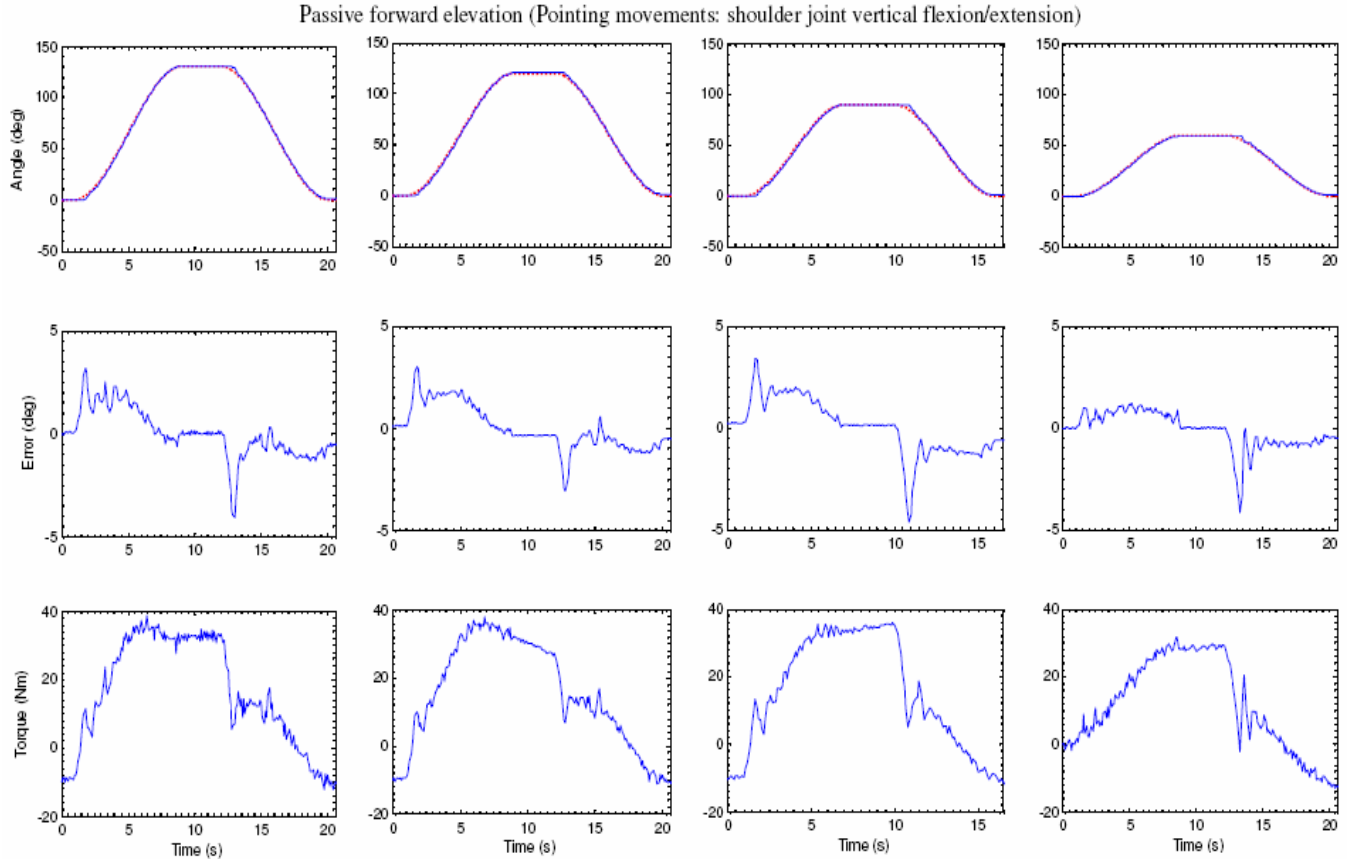

Figure 16 Passive arm movement along transverse plane, (a) shoulder joint horizontal flexion/extension (b) shoulder joint, vertical flexion motion, up to 90° and maintain that position while performing shoulder joint horizontal flexion/extension motion (see online version for colours)

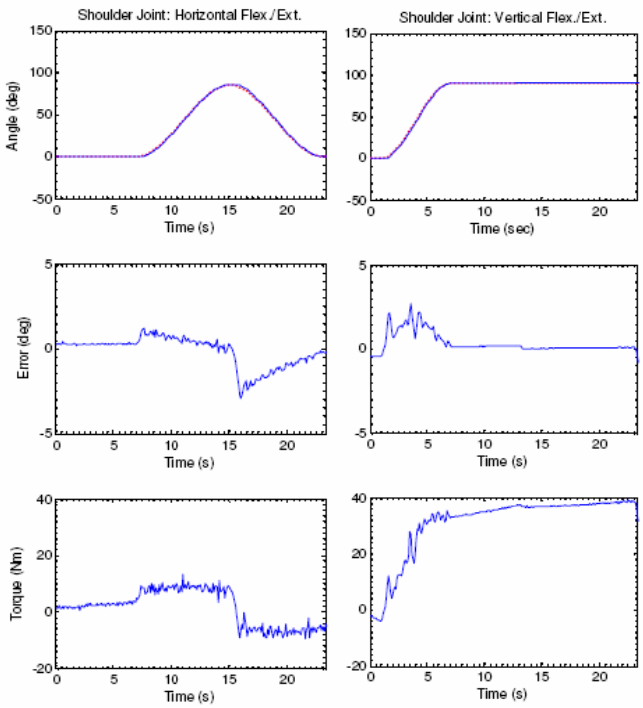

(a) (b)

Figure 17 Passive arm therapy, a cooperative movement of shoulder (internal/external rotation) and elbow joint motion, (a) elbow joint, flexion motion/extension motion (b) repetitive movement of shoulder joint internal/external rotation (see online version for colours)

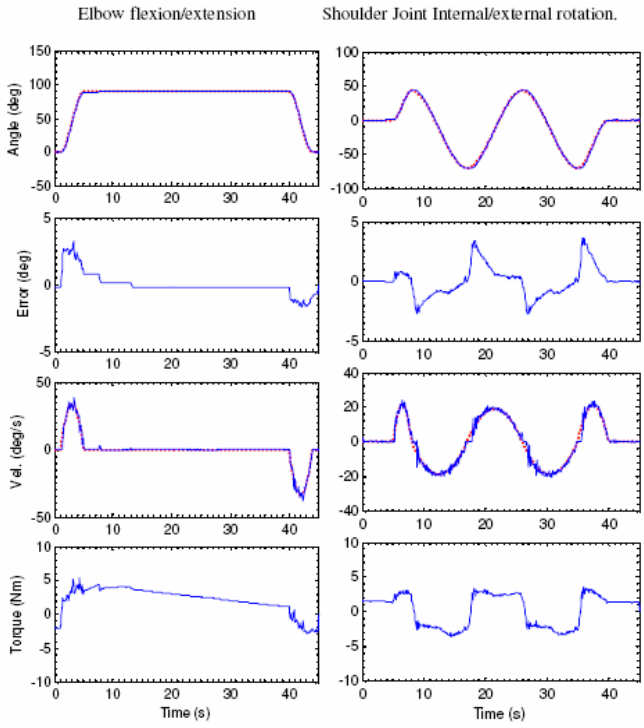

(a) (b)

Reaching movements are widely used and recommended for multi joint movement exercises. A repetitive straight ahead reaching movement is depicted in Figure 18, where the subject supposed to slide his or her hand gently over the surface of a table with the elbow initially at 90°. This movement is similar to dusting a table, which involves simultaneous and repetitive rotation at the elbow (extension) and shoulder joints. Typically this exercise is repeated ~10 times (Brigham and Women's Hospital, 2010), therefore a few repetitions are depicted in Figure 18.

Figure 18 Reaching movement, straight ahead, cooperative and combine movement of shoulder and elbow joint, (a) shoulder joint vertical flexion/extension (b) elbow flexion/extension (see online version for colours)

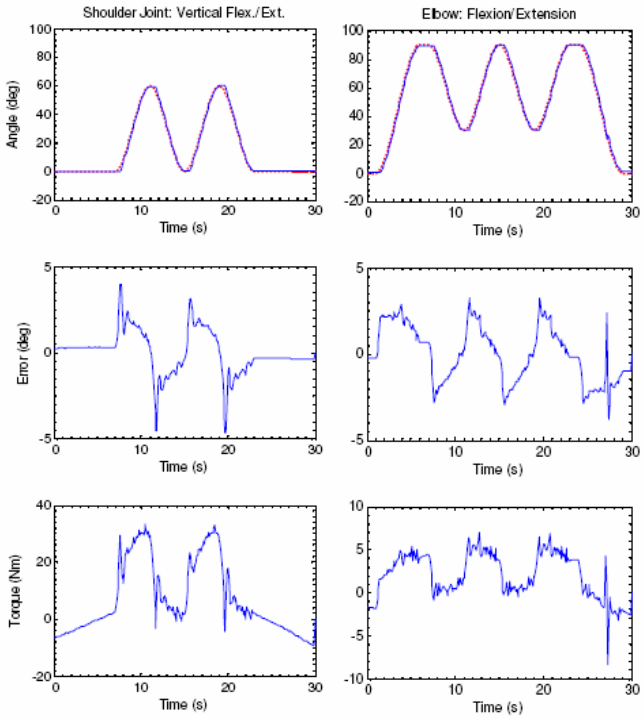

(a) (b)

As depicted from Figures 15 to 18 the maximum tracking deviation was observed to be around 2.5°, with a maximum steady state position error of around 0.1°.

5.1.2 Passive therapy using the mExoArm

The experimental results with the *mExoArm* for shoulder joint horizontal flexion/extension and internal/external rotation are depicted in Figures 19 and 20, respectively. In those tasks, the subject (robot user) operates the *mExoArm* with his/her left hand to perform repetitive movement. It is seen from the top most plots that the desired trajectories (solid line) overlapped with the measured ones (dotted line). The tracking error also in this case was found to be quite small (<4°).

Figure 19 Shoulder joint horizontal and vertical flexion/extension motion by *mExoArm*, (a) repetitive movement of shoulder joint horizontal flexion/extension (b) shoulder joint vertical flexion/extension (see online version for colours)

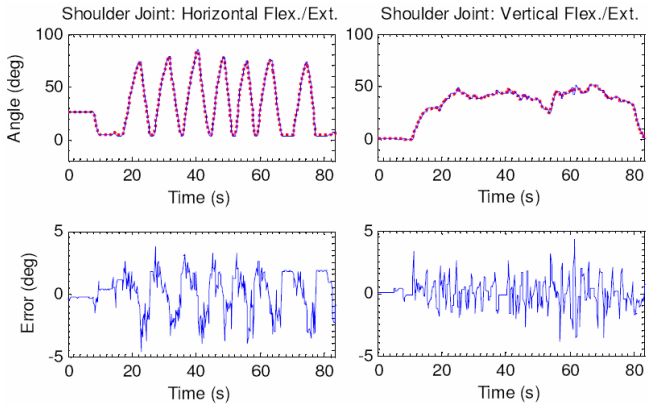

(a) (b)

Figure 20 Passive rehabilitation by *mExoArm*, combine shoulder and elbow joint movement, (a) shoulder joint internal external rotation (b) elbow flexion/extension (see online version for colours)

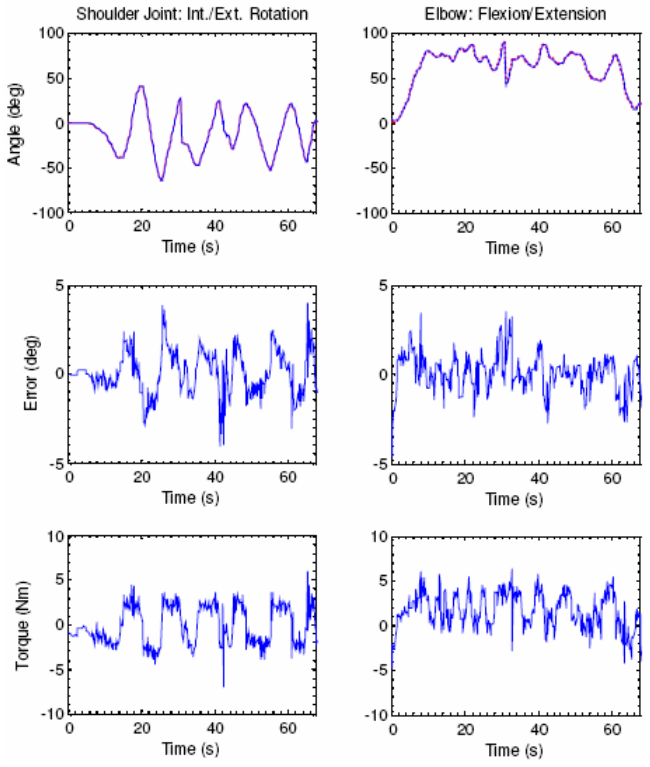

(a) (b)

To further evaluate the performance of the *mExoArm*, repetitive elbow flexion/extension movements were performed at various speeds. Experimental results for these exercises are illustrated in Figure 21. The results demonstrate excellent tracking performance of the controller even for the varying speed of movement.

Finally, a cooperative motion of elbow and shoulder joint movement using the *mExoArm* is shown in Figure 22. The results reveal that in all cases (Figures 21 and 22) the measured trajectory overlapped with the desired trajectory, and thus guarantees the performance of effective passive rehabilitation.

Using the *mExoArm* is an alternative way to provide passive therapy as well as to provide motion assist. Moreover, the *mExoArm* could potentially be used to tele-operate the *ExoRob*.

Figure 21 Repetitive, elbow flexion/extension by *mExoArm* (see online version for colours)

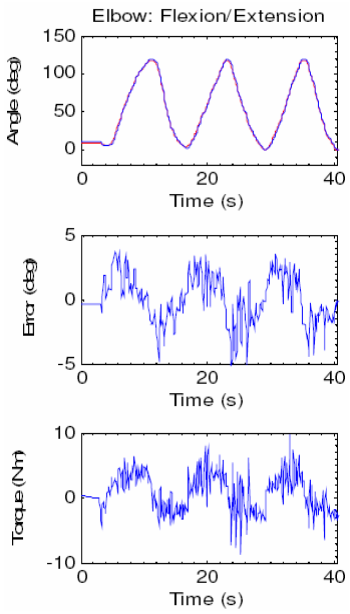

Figure 22 Reaching movement by *mExoArm*, (a) shoulder joint vertical flexion/extension movement (b) elbow flexion/extension (see online version for colours)

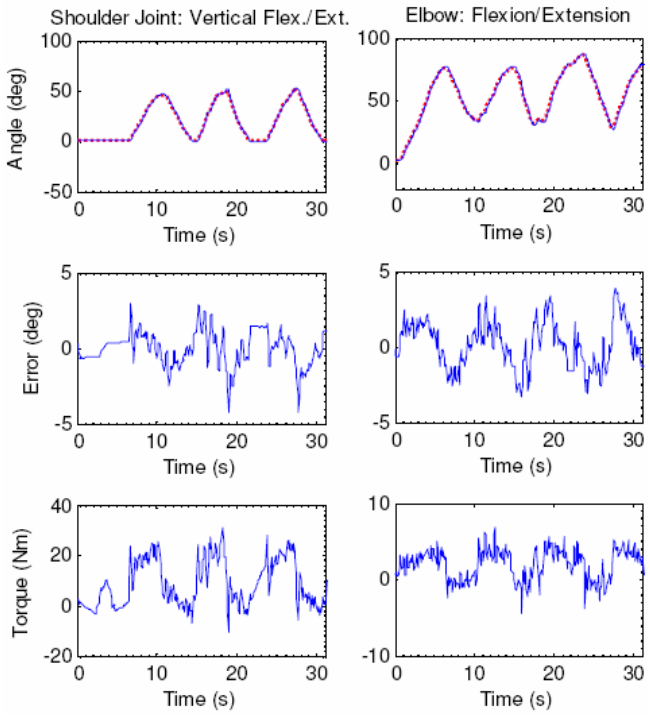

(a) (b)

5.2 Experimental results with compliance control

Figure 23 shows the results obtained with the compliance control for elbow joint flexion/extension [Figure 23(a)] and shoulder joint internal/external rotation [Figure 23(b)]. It can be seen in Figure 23 that this control approach (compliance control with gravity compensation) gives better tracking performance compared to the PID control technique. Note that for the same passive exercises, the maximum tracking error was around 2.5° with the PID control technique, whereas with compliance control it was around 0.5° [compare Figure 23 with Figures 18(b) and 17(b)].

Figure 23 (a) Elbow flexion/extension (b) shoulder joint internal/external rotation (see online version for colours)

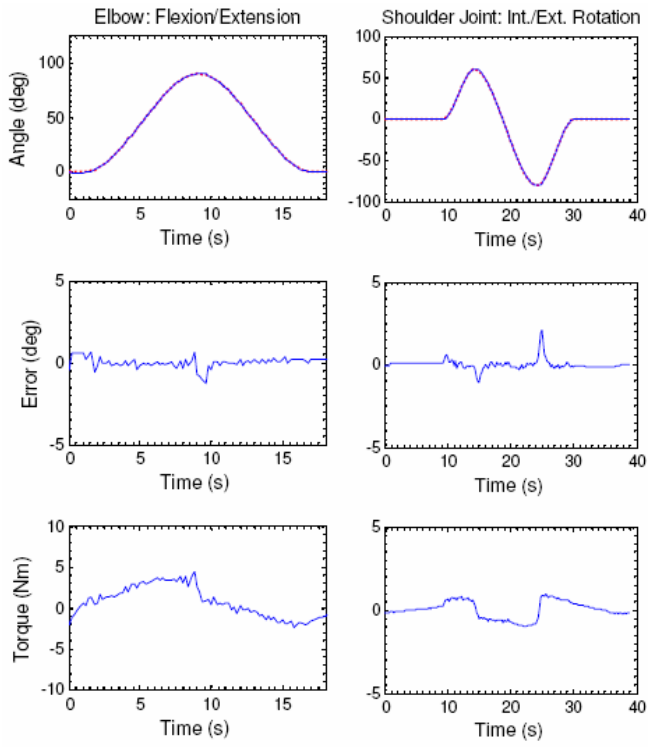

(a) (b)

To further evaluate the performance of the compliance control technique and also to show some compliance nature of the controller, an experiment was carried out where the subject is directed to push the wrist handle (i.e., X, Y, and Z directions with respect base frame) while the *ExoRob* is at the steady state position, maintaining the elbow joint angle at 90° against gravity (see topmost plot of Figure 24). The 2nd row of Figure 24 compares the desired positions of the wrist joint (dotted line) to the measured position (solid line) of wrist joint in Cartesian space. It is obvious from the figure that the end-effector exhibits some spring characteristics along the Cartesian degree of freedom (Figure 24, last two rows).

Comparing the natural variability of human arm movement (Laurette et al., 2005; Beers et al., 2004; Sanger, 2000; Buneo et al., 1995; Song et al., 2011; Meyer et al., 1988) with these results, we may conclude that the *ExoRob* can efficiently track the desired trajectories, and thus should be adequate for the purpose of performing passive arm movement therapy.

Experimental results thus validated the developed model and also evaluated the performance of the *ExoRob* with regard to trajectory tracking. Note that, the control gains used for the experiments were found by trial and error, and are as follows:

$$K_P = diag[275\ 275\ 90\ 70],\ K_V = diag[30\ 35\ 5\ 10]$$

$$K_I = diag[75\ 290\ 30\ 30],\ K_{px} = diag[20\ 20\ 20\ 60\ 60\ 60]$$

$$K_v = diag[10\ 50\ 10\ 60],\ K_i = diag[10\ 150\ 10\ 200].$$

Figure 24 Stiffness characteristics of the end-effector (see online version for colours)

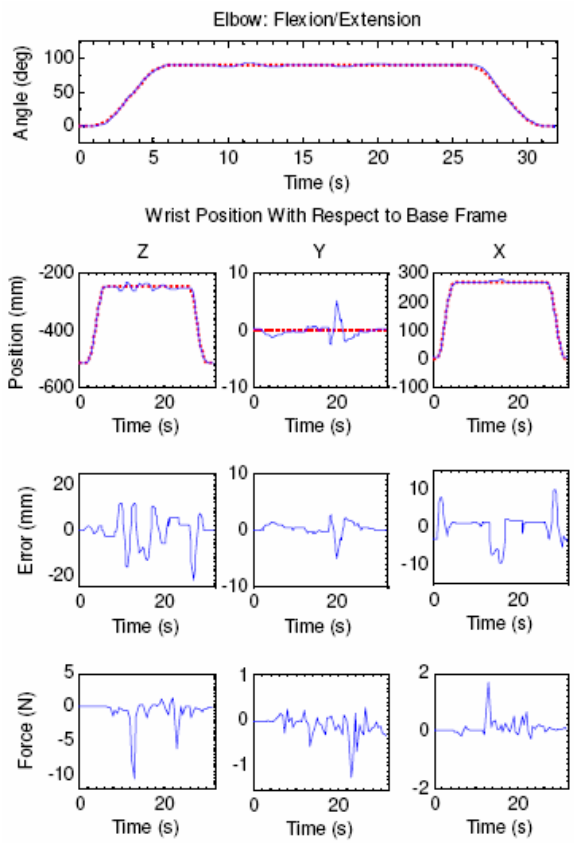

6 Conclusions

A 4DoFs exoskeleton robot corresponding to human shoulder and elbow joint movements has been developed to provide effective rehabilitation for physically disabled individuals, with impaired upper-limb function. The kinematic model of the proposed exoskeleton robot was also presented. Mechanical and actuation mechanism of the *ExoRob* was described. Experiments were carried out to evaluate the performance of the *ExoRob*, where typical passive rehabilitation exercises for single and multi joint movements of the upper-limb were performed (with the pre-programmed trajectory tracking approach and also with master exoskeleton arm). Experimental results show that the

ExoRob was able to provide effective rehabilitation for the shoulder (in 3DoFs: horizontal and vertical flexion/extension, and internal-external rotation) and elbow joint (1DoF: flexion/extension) movements.

Current work in-progress includes controlling the *ExoRob* with non-linear techniques (sliding mode control technique). Future work will include the development of an electromyogram (EMG)-based controller to control the *ExoRob* as well as to provide VR-based 'active rehabilitation' (Song et al., 2011). Note that EMG signal is biologically generated and it reflects the user's true intention of motions (Kiguchi et al., 2003; Wu and Chen, 2011). Therefore, skin surface EMG signals will be used for the real time control of the *ExoRob*.

Acknowledgements

The first author gratefully acknowledges the support provided for this research through a FQRNT-V1 scholarship.

References

Alexander, M.A., Nelson, M.R. and Shah, A. (1992) 'Orthotics, adapted seating and assistive device', in *Pediatric Rehabilitation*, 2nd ed., Williams and Wilkins, Baltimore, MD, pp.186–187.

Allen, J.R., Karchak, A., Jr. and Bontrager, E.L. (1972) 'Final project report, design and fabricate a pair of Rancho anthropomorphic manipulator', Technical report, The Rancho Los Amigos Hospital Inc., 12826, Hawthorm Street, Downey CA.

Alvarez-Ramirez, J., Cervantes, I. and Kelly, R. (2000) PID regulation of robot manipulators: stability and performance', *Systems & Control Letters*, Vol. 41, No. 2, pp.73–83.

Beers, R.J.V., Haggard, P. and Wolpert, D.M. (2004) 'The role of execution noise in movement variability', *Journal of Neurophysiology*, Vol. 91, No. 2, pp.1050–1063.

Brigham and Women's Hospital (2010) 'Physical therapy standards of care and protocols', available at http://www.brighamandwomens.org/RehabilitationServices/StandardsofCare.aspx?sub=1 (accessed on 23 February 2012)

Brose, S.W., Weber, D.J., Salatin, B.A., Grindle, G.G., Wang, H., Vazquez, J.J. and Cooper, R.A. (2010) 'The role of assistive robotics in the lives of persons with disability', *Am. J. Phys. Med. Rehabil.*, Vol. 89, No. 6, pp.509–521.

Buneo, C.A., Boline, J., Soechting J.F. and Poppele, R.E. (1995) 'On the form of the internal model for reaching', *Experimental Brain Research*, Vol. 104, No. 3, pp.467–479.

Burgar, C.G., Lum, P.S., Shor, P.C. and Van der Loss, H.F.M. (2000) 'Development of robots for rehabilitation therapy: the Palo Alto VA/Stanford experience', *Journal of Rehabilitation Research and Development*, Vol. 37, No. 6, pp.663–673.

Colombo, R., Pisano, F., Micera, S., Mazzone, A., Delconte, C., Carrozza, M.C., Dario, P. and Minuco, G. (2005) 'Robotic techniques for upper limb evaluation and rehabilitation of stroke patients', *IEEE Transactions on Neural Systems and Rehabilitation Engineering*, Vol. 13, No. 3, pp.311–324.

Craig, J.J. (2005) *Introduction to Robotics: Mechanics and Control*, 3rd ed., Pearson/Prentice Hall, Upper Saddle River, NJ.

Craig, R.C., Jonathan, T. and Stephen, N.R. (2009) 'Development of an exoskeleton haptic interface for virtual task training', Paper presented at the *IEEE/RSJ International Conference on Intelligent Robots and Systems*, pp.3697–3702.

Culmer, P.R., Jackson, A.E., Makower, S., Richardson, R., Cozens, J.A., Levesley, M.C. and Bhakta, B.B. (2010) 'A control strategy for upper limb robotic rehabilitation with a dual robot system', *IEEE/ASME Transactions on Mechatronics*, Vol. 15, No. 4, pp.575–585.

De Luca, A., Siciliano, B. and Zollo, L. (2005) 'PD control with online gravity compensation for robots with elastic joints: theory and experiments', *Automatica*, Vol. 41, No. 10, pp.1809–1819.

Frisoli, A., Salsedo, F., Bergamasco, M., Rossi, B. and Carboncini, M.C. (2009) 'A force feedback exoskeleton for upper limb rehabilitation in virtual reality', *Applied Bionics and Biomechanics*, Vol. 6, No. 2, pp.115–126.

Garrec, P., Friconneau, J.P., Measson, Y. and Perrot, Y. (2008) 'ABLE, an innovative transparent exoskeleton for the upper-limb', Paper presented at the *IEEE/RSJ International Conference on Intelligent Robots and Systems*, pp.1483–1488.

Gopura, R.A.R.C., Kiguchi, K. and Yang, L. (2009) 'SUEFUL-7: a 7DOF upper-limb exoskeleton robot with muscle-model-oriented EMG-based control', Paper presented at the *2009 IEEE/RSJ International Conference on Intelligent Robots and Systems (IROS 2009)*, 11–15 October, Piscataway, NJ, USA.

Gupta, A. and O'Malley, M.K. (2006) 'Design of a haptic arm exoskeleton for training and rehabilitation', *IEEE/ASME Transactions on Mechatronics*, Vol. 11, No. 3, pp.280–289.

Hallaceli, H., Manisali, M. and Gunal, I. (2004) 'Does scapular elevation accompany glenohumeral abduction in healthy subjects?', *Arch. Orthop. Trauma Surg.*, Vol. 124, No. 6, pp.378–381.

Heart and Stroke Foundation (2009) *Stroke Rehabilitation*, available at http://www.heartandstroke.com/site/c.ikIQLcMWJtE/b.3484221/k.467D/Stroke___Stroke_Rehabilitation.htm (accessed on 23 February 2012)

Hillman, S.K. (2003) *Interactive Functional Anatomy-DVD*, Primal Pictures Ltd., London.

Homma, K. and Arai, T. (1995) 'Design of an upper limb assist system with parallel mechanism', Paper presented at the *IEEE International Conference on Robotics and Automation*, pp.1302–1307.

Inverarity, L. (2008) 'Exercises to strengthen the elbow', available at http://physicaltherapy.about.com/od/strengtheningexercises/a/Elbowex.htm (accessed 23 February 12)

Johnson, G.R. and Buckley, M.A. (1997) 'Development of a new motorised upper limb orthotic system (MULOS)', in *Proceedings of RESNA '97. Lets Tango – Partnering People and Technologies*, 20–24 June, Arlington, VA, USA, RESNA Press, pp.399–401.

Kiguchi, K., Iwami, K., Yasuda, M., Watanabe, K. and Fukuda, T. (2003) 'An exoskeletal robot for human shoulder joint motion assist', *IEEE/ASME Transactions on Mechatronics*, Vol. 8, No. 1, pp.125–135.

Krebs, H.I., Volpe, B.T., Aisen, M.L. and Hogan, N. (2000) 'Increasing productivity and quality of care: robot-aided neuro-rehabilitation', *Journal of Rehabilitation Research and Development*, Vol. 37, No. 6, pp.639–652.

Laurette, H., Chantal, B., Carole, F., Isabelle, O. and Michelle F. (2005) 'Role of proprioceptive information in movement programming and control in 5 to 11-year old children', *Human Movement Science*, Vol. 24, No. 2, pp.139–154.

Loureiro, R., Amirabdollahian, F., Topping, M., Driessen, B. and Harwin, W. (2003) 'Upper limb robot mediated stroke therapy – GENTLE/s approach', *Autonomous Robots*, Vol. 15, No. 1, pp.35–51.

Luttgens, K. and Hamilton, N. (1997) *Kinesiology: Scientific Basis of Human Motion*, 9th ed., Brown & Benchmark, Madison, WI.

Mackay, J. and Mensah, G. (2004) *Atlas of Heart Disease and Stroke*, World Health Organization, Nonserial Publication, Brighton, UK.

Masia L., Krebs, H.I., Cappa, P. and Hogan, N. (2007) 'Design and characterization of hand module for whole-arm rehabilitation following stroke', *IEEE/ASME Transactions on Mechatronics*, Vol. 12, No. 4, pp.399–407.

Meyer, D.E., Abrams, R.A., Kornblum, S., Wright, C.E. and Smith, J.E.K. (1988) 'Optimality in human motor performance: ideal control of rapid aimed movements', *Psychological Review*, Vol. 95, No. 3, pp.340–370.

Moeslund, T.B., Madsen, C.B. and Granum, E. (2005) 'Modelling the 3D pose of a human arm and the shoulder complex utilising only two parameters', *Integrated Computer-Aided Engineering*, Vol. 12, pp.159–175.

National Instruments (2010) 'NI cRIO-9074 – integrated 400 MHz real-time controller and 2M gate FPGA', available at http://sine.ni.com/nips/cds/view/p/lang/en/nid/203964 (accessed on 23 February 2012).

Nef, T., Guidali, M., Klamroth-Marganska, V. and Riener, R. (2009) 'ARMin – exoskeleton robot for stroke rehabilitation', Paper presented at the *11th International Congress of the IUPESM. Medical Physics and Biomedical Engineering. World Congress 2009, Neuroengineering, Neural Systems, Rehabilitation and Prosthetics*, 7–12 September, Berlin, Germany.

Noritsugu, T. and Tanaka, T. (1997) 'Application of rubber artificial muscle manipulator as a rehabilitation robot', *IEEE/ASME Transactions on Mechatronics*, Vol. 2, pp.259–267.

Parker, V.M., Wade, D.T. and Langton, H.R. (1986) 'Loss of arm function after stroke: measurement, frequency, and recovery', *Int. Rehabilitation Medicine*, Vol. 8, No. 2, pp.69–73.

Perry, J.C., Rosen, J. and Burns, S. (2007) 'Upper-limb powered exoskeleton design', *IEEE/ASME Transactions on Mechatronics*, Vol. 12, pp.408–417.

Prange, G.B., Jannink, M.J., Groothuis-Oudshoorn, C.G., Hermens, H.J. and Ijzerman, M.J. (2006) 'Systematic review of the effect of robot-aided therapy on recovery of the hemiparetic arm after stroke', *J. Rehabil. Res. Dev.*, Vol. 43, pp.171–184.

Rahman, M.H., Saad, M., Kenne, J.P. and Archambault, P.S. (2009) 'Modeling and control of a 7DOF exoskeleton robot for arm movements', Paper presented at the *2009 IEEE International Conference on Robotics and Biomimetics (ROBIO 2009)*, 19–23 December, Guilin, China.

Rahman, M.H., Saad, M., Kenné, J.P. and Archambault, P.S. (2010) 'Modeling and development of an exoskeleton robot for rehabilitation of wrist movements', Paper presented at the *IEEE/ASME International Conference on Advanced Intelligent Mechatronics*, Montreal, Canada, July, pp.25–30.

Rahman, T., Sample, W., Seliktar, R., Alexander, M. and Scavina, M. (2000) 'A body-powered functional upper limb orthosis', *Journal of Rehabilitation Research and Development*, Vol. 37, No. 6, pp.675–680.

Rocco, P. (1996) 'Stability of PID control for industrial robot arms', *IEEE Transactions on Robotics and Automation*, Vol. 12, No. 4, pp.606–614.

Salisbury, J.K. (1980) 'Active stiffness control of a manipulator in Cartesian coordinates', Paper presented at the *19th IEEE Conference on Decision and Control*, pp.95–100.

Sanchez, R.J., Wolbrecht, E., Smith, R., Liu, J., Rao, S., Cramer, S., Rahman, T., Bobrow, J.E. and Reinkensmeyer, D.J. (2005) 'A pneumatic robot for re-training arm movement after stroke: rationale and mechanical design', Paper presented at the *2005 IEEE 9th International Conference on Rehabilitation Robotics*, 28 June–1 July, Piscataway, NJ, USA.

Sanger, T.D. (2000) 'Human arm movements described by a low-dimensional superposition of principal components', *The Journal of Neuroscience*, Vol. 20, No. 3, pp.1066–1072.

Schilling, R.J. (1990) *Fundamental of Robotics: Analysis and Control*, Prentice Hall, Englewood Cliffs, NJ.

Song, Z., Guo, S. and Fu, Y. (2011) 'Toward the identification of EMG-signal and its bio-feedback application', *International Journal of Mechatronics and Automation*, Vol. 1, No. 1, pp.19–28.

Soslowsky, L.J., Flatow, E.L., Bigliani, L.U. and Mow, V.C. (1992) 'Articular geometry of the glenohumeral joint', *Clinical Orthopaedics and Related Research*, Vol. 285, pp.181–190.

Takahashi, C.D., Der-Yeghiaian, L., Le, V., Motiwala, R.R. and Cramer, S.C. (2008) 'Robot-based handmotor therapy after stroke', *Brain*, Vol. 131, No. 2, pp.425–437.

Trafton, A. (2010) 'Robotic therapy helps stroke patients regain functions', available at http://www.physorg.com/news190880394.html (accessed on 23 February 2012).

Tsagarkis, N.G. and Caldwell, D.G. (2003) 'Development and control of a soft-actuated exoskeleton for use in physiotherapy and training', *Autonomous Robots*, pp.15–21.

Volpe, B.T, Krebs, H.I. and Hogan, N. (2003) 'Robot-aided sensorimotor training in stroke rehabilitation', *Adv. Neurol*., Vol. 92, pp.429–433.

Volpe, B.T., Krebs, H.I., Hogan, N., Edelsteinn, L., Diels, C.M. and Aisen, M.L. (1999) 'Robot training enhanced motor outcome in patients with stroke maintained over 3 years', *Neurology*, Vol. 53, pp.1874–1876.

Wilson, S.R and Price, D.D. (2009) *Dislocation Shoulder*, available at http://emedicine.medscape.com/article/823843-overview (accessed on 23 February 2012).

Winter, A.D. (1992) *Biomechanics and Motor Control of Human Movements*, 2nd ed., University of Waterloo Press, Canada.

Wu, Y.C., and Chen, J.S. (2011) 'Toward the identification of EMG-signal and its bio-feedback application', *International Journal of Mechatronics and Automation*, Vol. 1, No. 2, pp.112–120.

Yang, C., Han, J., Peter, O.O. and Huang, Q. (2011) 'PID control with gravity compensation for hydraulic 6-DOF parallel manipulator', in T. Mansour (Ed.): *PID Control, Implementation and Tuning*, p.238, InTech.

Zatsiorsky, V. and Seluyanov, V. (1983) 'The mass and inertia characteristics of the main segments of the human body', *Biomechanics*, VIII-B, Vol. 56, No. 2, pp.1152–1159.